



ISSN: 1813-162X (Print); 2312-7589 (Online)

Tikrit Journal of Engineering Sciences

available online at: <http://www.tj-es.com>

TJES

Tikrit Journal of
Engineering Sciences

An Experimental and Numerical Investigation of the Effect of Different Wall Types on the Iraqi Building's Thermal Load

Atif Ali Hasan ^{id}^a, Mahmood H. Khaleel ^{id}^{b*}, Kadhum Auda Jhehf ^{id}^c^a Technology Institute –Baghdad, Middle Technical University, Iraq.^b Technical Institute –Kirkuk, Northern Technical University, Iraq.^c Technical Engineering College – Baghdad, Middle Technical University, Iraq.**Keywords:**

Building Load Reduction; Building Materials; Drilled Concrete; Electrical Level Reduction; Thermal Building Loads.

Highlights:

- Four wall models Created to limit heat transmission by covering the building's outside wall.
- Experimental investigation of perforated concrete blocks with holes. A numerical model was also created utilizing computational analysis.
- The key objective of perforated blocks used to cover facades is to reduce heat gain from the environment, which will reduce energy consumption for air conditioning.

ARTICLE INFO**Article history:**

Received	12 June	2023
Received in revised form	22 July	2023
Accepted	16 Oct.	2023
Final Proofreading	16 Dec.	2023
Available online	10 Mar.	2024

© THIS IS AN OPEN ACCESS ARTICLE UNDER THE CC BY LICENSE. <http://creativecommons.org/licenses/by/4.0/>

Citation: Hasan AA, Khaleel MH, Jhehf KA. An Experimental and Numerical Investigation of The Effect of Different Wall Types on the Iraqi Building's Thermal Load. *Tikrit Journal of Engineering Sciences* 2024; 31(1): 223-235.

<http://doi.org/10.25130/tjes.31.1.19>

***Corresponding author:**

Mahmood H. Khaleel



Technical Institute –Kirkuk, Northern Technical University, Iraq.

Abstract: The study aims to reduce heat transfer in a building's conditioned space due to high environmental temperatures in the summer. The heat transfer through the building's external walls increases the need for electrical energy. This study developed four models to reduce heat transfer by covering the exterior wall of the building with perforated concrete blocks with holes, whose diameters varied within the range of 6–10 mm, distributed in three rows of variable hole diameter, each row containing three holes of equal diameter: Model A1 (the diameter of the three holes in the first row was 6 mm, and the diameter of the three holes in the second row was 8 mm, while the diameter of the three holes in the third row was 10 mm). Model A2: The hole arrangement with the sequence 10, 8, and 6 mm. Model B1: The hole arrangement was with the sequence 6, 10, and 8 mm. Model B2: The hole arrangement was with the sequence 8, 10, and 6 mm. The study examined the air gap between the building's covering blocks and the original wall. A thermal test room was built with an air conditioner and a cumulative electric energy meter to measure energy consumption. Perforated block models covered the test room's wall. Also, a numerical model was prepared using the ANSYS-Fluent package v. 16.2. The experimental and numerical results were consistent. Model B1 achieved higher electrical seasonal consumption than the conventional model, about 98.5 kilowatt-hours. While the other four models recorded low energy consumption, i.e., model A1 consumed 87.5 kilowatt-hours, with a reduction of 11.2%; model A2 consumed 83.9 kilowatt-hours, with a reduction of 15%; model B2 consumed 80 kilowatt-hours, with a reduction of 19%; and model B1 consumed 78 kilowatt-hours, with a reduction of 21%.

تحقيق تجريبي وعددي في تأثير أنواع الجدران المختلفة على الحمل الحراري للمبنى العراقي

عاطف علي حسن^١، محمود حسين خليل^٢، كاظم عودة جحف^٣

^١ قسم تقنيات ميكانيك القدرة / معهد التكنولوجيا - بغداد/ الجامعة التقنية الوسطى / العراق.

^٢ قسم تقنيات ميكانيك القدرة / المعهد التقني- كركوك/ الجامعة التقنية الشمالية/ العراق.

^٣ قسم تقنيات الوقود والطاقة /الكلية التقنية الهندسية – بغداد/ الجامعة التقنية الوسطى/العراق.

الخلاصة

تهدف الدراسة إلى تقليل انتقال الحرارة في الحيز المكيف للمبنى بسبب ارتفاع درجات الحرارة البيئية الخارجية في فصل الصيف. ويرجع ذلك إلى انتقال الحرارة عبر الجدران الخارجية للمبنى، مما يؤدي إلى زيادة في استهلاك الطاقة الكهربائية. ونتيجة لذلك، قامت هذه الدراسة بتطوير أربعة نماذج للجدران لتقليل كمية انتقال الحرارة من خلال تغطية الجدار الخارجي للمبنى بالكتل الخرسانية المثقبة بتراوح أقطار الثقوب بين 6-10 ملم، موزعة على ثلاثة صفوف متغيرة الاقطار. كل صف يحتوي على ثلاث فتحات متساوية القطر: النموذج A1 (قطر الثقوب الثلاثة في الصف الأول 6 ملم و قطر الثقوب الثلاثة في الصف الثاني 8 ملم، بينما قطر الثقوب الثلاثة في الصف الثالث 10 ملم)، أما في النموذج الثاني A2، فقد أخذ ترتيب الثقوب التسلسل 10، 8، 6 ملم، وفي النموذج الثالث B1، اتخذ ترتيب الثقوب التسلسل 6، 10، 8 ملم، بينما وفي النموذج الرابع B2، أخذ ترتيب الثقوب التسلسل 8، 10، 6 ملم. تناولت الدراسة تأثير فتح و غلق الفجوة الهوائية بين جدران التغليف للمبنى والجدار الأصلي، وتم بناء غرفة اختبار حراري مزودة بمكيف هواء ومقياس طاقة كهربائية تراكمية لقياس استهلاك الطاقة. تم استخدام نماذج الجدران المثقبة لتغطية الجدار الاصلي لغرفة الاختبار، كما تم إعداد نموذج عددي باستخدام برنامج ANSYS-Fluent الإصدار 16.2. وتوافقت النتائج العملية مع نتائج التحليل العددي، وحقق النموذج B1 أعلى تخفيض في الطاقة الحرارية عند مقارنة الاستهلاك الموسمي للطاقة الكهربائية المستهلكة لأغراض التكييف مع النموذج التقليدي والذي يبلغ حوالي 98.5 كيلووات/ساعة، فيما سجلت النماذج الأربعة المطورة استهلاك الطاقة بنسب تخفيض: النموذج A1 سجل 87.5 كيلووات/ساعة و بنسبة انخفاض 11.2٪؛ موديل A2 سجل 83.9 كيلووات/ساعة و بتخفيض 15٪؛ والنموذج B2 سجل 80 كيلووات/ساعة و بتخفيض 19٪؛ والنموذج B1 بقدرة 78 كيلووات/ساعة بتخفيض 21٪.

الكلمات الدالة: تخفيض أحمال البناء، مواد البناء، الخرسانة المحفورة، تخفيض المستوى الكهربائي، أحمال البناء الحرارية.

1. INTRODUCTION

Concrete blocks are increasingly being used in construction in Iraq as a substitute for pottery bricks, which undermines the geographical area of agricultural land. The increasing implementation of buildings in a structural shape led to the use of solid and hollow concrete blocks for masonry that has a high density of (1200 to 2400 kg/m³) and a high thermal conductivity of (1.8 to 3) W/m.K [1] instead of bricks due to economic and environmental reasons. The problem of increasing cooling loads for those buildings becomes apparent and increases electrical energy consumption. The energy spent for conditioning buildings is estimated to be nearly 70% of the total annual energy consumed per family [2]. Therefore, improving the thermal performance of the building blocks becomes essential in demonstrating the energy consumed. The wall materials' density is considered one of the most significant physical characteristics due to its direct impact on the material's thermal conductivity, heat capacity, and thermal storage. Through it, the thermal performance evaluation of walls indicates that a thick wall results in higher summer month energy savings than a thin wall [3,4]. Many research efforts acknowledged many solutions. The following are some proposed solutions:

- Increasing the total structural thermal resistance value [5–8] was achieved by utilizing insulation within the gap of the construction material with a thickness of (65 mm), reducing the overall coefficient of heat transfer from (2.39) to (0.49) W/m².K [9].

- Maintaining a closed air gap within the wall components [10].
- Studying the optimum air gap for a selected insulation. Using optimal thicknesses of different insulation materials and having air gaps of 2 cm, 4 cm, and 6 cm reduce energy consumption and emissions by 65-77 % compared to a wall without insulation or air gaps [11].
- Using a heavy internal wall with a ventilated air gap to store solar energy Utilizing an internal wall to store solar energy reduces heat demand in the winter. It improves thermal comfort in the summer because thermal mass increases and airflow cools the internal wall at night [12].
- Propelling moist air into the wall gap to absorb more accumulated heat (sensible and latent heat) before transmitting it to the interior space. The reduction in electrical power reaches about 50%, as well as the use of the open courtyard to recycle air and provide building ventilation [13].

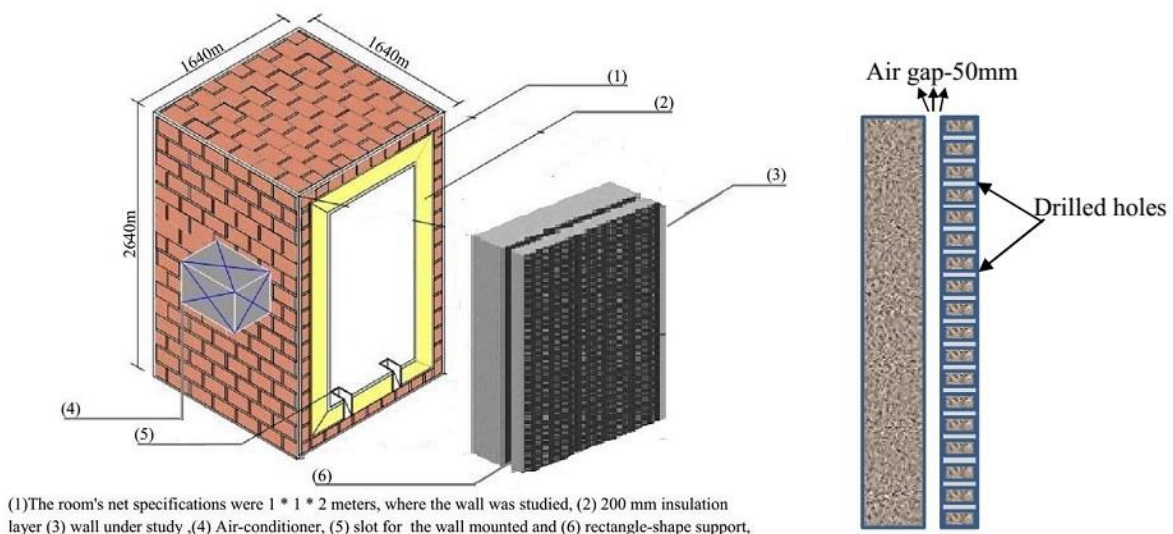
Furthermore, recycled materials from industry, agriculture, and natural waste can be combined with cement mortar to reconstruct new building materials with low thermal conductivity and density [14]. The recycled materials can be reused immediately or after processing. The result is lightweight cement, environmentally friendly, and sustainable products. Also, natural aggregates can be replaced with recyclable materials, such as waste plastic, fly ash, and silica fume, then mixed with cement mortar to improve compressive strength.

Crushed waste glass powder can be mixed with cement mortar to improve mechanical resistance. Waste eggshells can be mixed with soil and cement bricks to produce excellent technical building materials properties. Also, mixing rice straw with cement mortar reduces greenhouse gas emissions and energy consumption and the compressive strength by 1% RH then increases from 2% to 3% RH before decreasing again [15–20]. The thermal loads can be reduced by reducing the solar heat load falling on the building, which depends on the building orientation, and covering its external roof, which reduces 54% of heat gain compared to an uncovered roof [21]. Complex finite Fourier transform (CFFT) is an analytical solution approach for estimating space heat gain through multilayer walls and flat roofs according to periodic boundary conditions. The CFFT technique is useful because it performs calculations for various multilayer wall and roof constructions and climatological locations with varying ambient air temperatures and solar heat inputs [22]. The cooling load temperature difference (CLTD) values for building walls and flat roofs are first determined using a periodic solution to the unsteady heat transfer issue. The disparities in CLTD values for Roof 2, Roof 13, and Wall 3 selected for principal directions fluctuate between 0 and 2.42 °C, 0 and 0.94 °C, and 1.8 and 4.3 °C, respectively. According to [23], the RTS (radiant time series) approach reveals that the variations between predicted heat gain estimates and those published in ASHRAE vary between 0 and 5 W/m². The ASHRAE standard data is used to validate numerical computations. Due to the Iraqi technology's simplicity and weak potential and the difficulty of applying any of these results to the building materials factory lines, the present study develops solid and perforated concrete

blocks currently used for external finishing purposes. The re-perforating blocks circulate ambient air through them and absorb part of the transferred heat, minimizing the overall heat absorption. The heat transferred by this block will be transferred to the other wall components, reducing the environmental impact of changing the room temperature. As a result, the energy consumption for air conditioning should be minimized.

2. MATERIAL AND METHOD

The present study aims to reduce heat transfer from the environment to the conditioned room. For this purpose, a (1×1×2 m) room was tested. The room is in Iraq's capital (Baghdad) (latitude 33,2 N°). One of the room walls, i.e., the test wall, was 1×2 m facing east. The other three walls were isolated with a 200mm-thick insulation. A window-type air conditioner was installed to maintain the room's design conditions (26,5 C). Fig. 1 shows the details of the room studied. The exterior wall coverings were cement blocks with 100 × 100 × 100 mm dimensions, used in Iraqi architecture. These blocks were drilled with various diameter drilling holes in each row. Four models were studied and evaluated, i.e., A1, A2, B1, and B2. A 50 mm air gap was left between the holes and the cement blocks that cover the wall. The dimensions of the pattern holes varied from model to model, with an average of three holes in each row and three rows in each model, as listed in Table 1. The wall with perforations Model A1 had three holes with a 6 mm diameter in the first row, three holes with an 8 mm diameter in the middle row, and three holes with a 10 mm diameter in the last row. The number of holes was the same for all models (A2, B1, and B2). However, the difference was the holes consequences, as shown in Fig. 2.



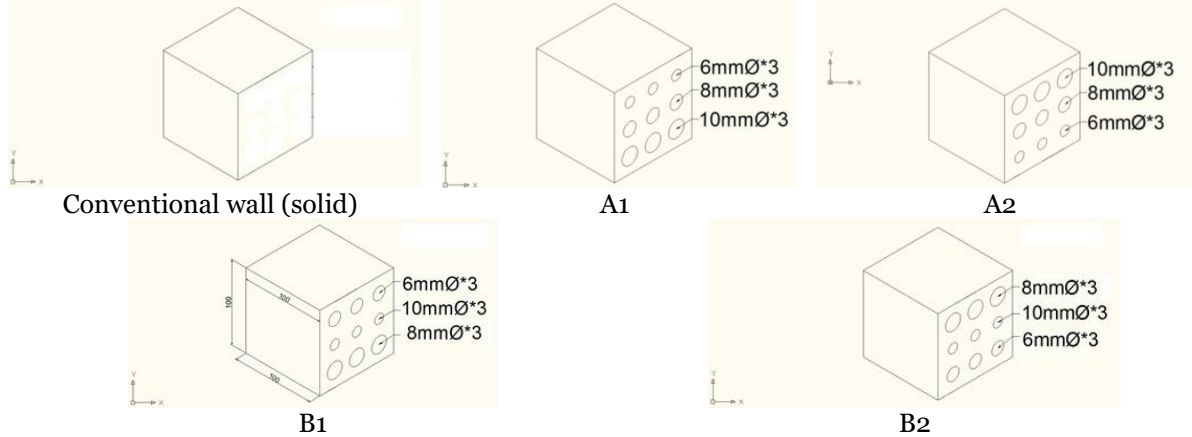
Test room specification

Studied wall Sectional view

Fig. 1 Sectional Test Room.

Table 1 Walls Models Characteristic.

Symbol	Total Number of Hole	Row Numbers	Column Number	Hole Matrix Description	Hole Diameter per Row
Model A1	9	3	3	Row1 Row2 Row3	6mmØ 8mmØ 10mmØ
Model A2	9	3	3	Row1 Row2 Row3	10mmØ 8mmØ 6mmØ
Model B1	9	3	3	Row1 Row2 Row3	6mmØ 10mmØ 8mmØ
Model B2	9	3	3	Row1 Row2 Row3	8mmØ 10mmØ 6mmØ

**Fig. 2** Wall Construction Models.

To investigate the thermal behavior of walls, the outside surface temperature of the building blocks (T_o) and the shaded area ambient air temperature (T_{sh}) were measured with a smart digital thermometer. While the wall interior surface temperature facing the building's conditioned space (T_i) and room air temperature (T_r) were measured with a pre-calibrated thermocouple thermometer. The total electrical energy consumption by the air conditioner was measured using period data readings by the cumulative power meter (Invendis ET-0054 20A Single Phase Energy Meter) on the 21st day of each summer month (May to September 2021). Data was collected from 6 a.m. to 7 p.m.

3. THEORETICAL MODELING ANALYSIS

It is evident that the analytical solution for the velocity and temperature distributions in an air gap inside a perforated wall, heated by constant heat flux from the exit and maintained at a uniform temperature from the intake, is not feasible. In instances of this kind, the analysis may be conducted by experimental methods or numerical techniques, such as the ANSYS-Fluent package version 16.2 [24]. Multiple variables are often present, and converting them into a small number of dimensionless quantities is customary. Using the Buckingham theorem, reducing the number of variables influencing a particular issue to a small set of dimensionless integers is possible. In the current scenario of natural convection, the

Rayleigh number (Ra) has significant importance since it quantitatively represents the ratio between buoyancy forces and viscous forces [25]:

$$Ra_H = \frac{g\beta\Delta TH^3}{\nu\alpha} \quad (1)$$

In the present scenario, the temperature disparity between the heated walls is utilized with the height H considered the pertinent spatial dimension. The driving forces of the natural convection are found in the numerator of the Rayleigh number, thereby establishing a positive correlation between the Rayleigh number and the intensity of the natural convection. Additionally, the resolution depends on the Prandtl number [22].

$$Pr = \frac{\mu c_p}{k} \quad (2)$$

The Prandtl number plays a significant role in the natural convection process, as it directly impacts the thickness of both the momentum and thermal boundary layers because heat serves as the primary driving factor for the momentum boundary layer. The Prandtl numbers often cited in the academic literature are those about water and air under atmospheric circumstances, which are around 7 and 0.7, respectively.

3.1. Governing Equations

A recommended first step would include considering the incompressible Navier-Stokes equations. The conservation forms of the partial differential equations (PDEs) controlling the system are as follows [25].

$$\frac{\partial u}{\partial t} + u\nabla u = -\frac{1}{\rho}\nabla p + \nu\nabla^2 u + g \quad (3)$$

Assuming that the gravitational vector is the only contributor to body forces. The property of incompressibility simplifies the continuity equation into the subsequent mathematical formula [25].

$$\nabla \cdot u = 0 \quad (4)$$

Considering the energy equation is necessary due to the influence of temperature changes on the flow [26].

$$\rho \frac{\partial E}{\partial t} + \rho \nabla \cdot (uH) = \rho u f + \nabla \cdot (\tau u) + \nabla \cdot (k\nabla T) + Q \quad (5)$$

It is important to note that, while the assumption of incompressibility is made, the influence of buoyant forces is considered by including a thermal expansion coefficient that generates the body force f . The equations may be reformulated into a generalized form, including a conserved variable. This reformulated system can then be solved using commercially available software, such as Fluent, using the finite volume approach [25]:

$$\frac{\partial \phi}{\partial t} + \nabla \cdot (\phi u) = \frac{1}{\rho} \nabla \cdot (\Gamma \nabla \phi) + \frac{1}{\rho} S_\phi \quad (6)$$

The equation above depicts the variable's temporal variation on the left side and the convective efflux of the fluid element. The equality arises from the relationship between the variable's growth, as influenced by diffusion and the volumetric source term, and is expressed on the right side of Eq. (6). The perforated suggested cement block thermal properties were measured in Baghdad Technology Institute Laboratories, while time lag (ϕ) and decrement factor were calculated using Eqs. (7) and (8) [27]:

$$\phi = t_{T_{in[max]}} - t_{T_{out[min]}} \quad (7)$$

$$Df = \frac{t_{T_{in[max]}} - t_{T_{in[min]}}}{t_{T_{out[max]}} - t_{T_{out[min]}}} \quad (8)$$

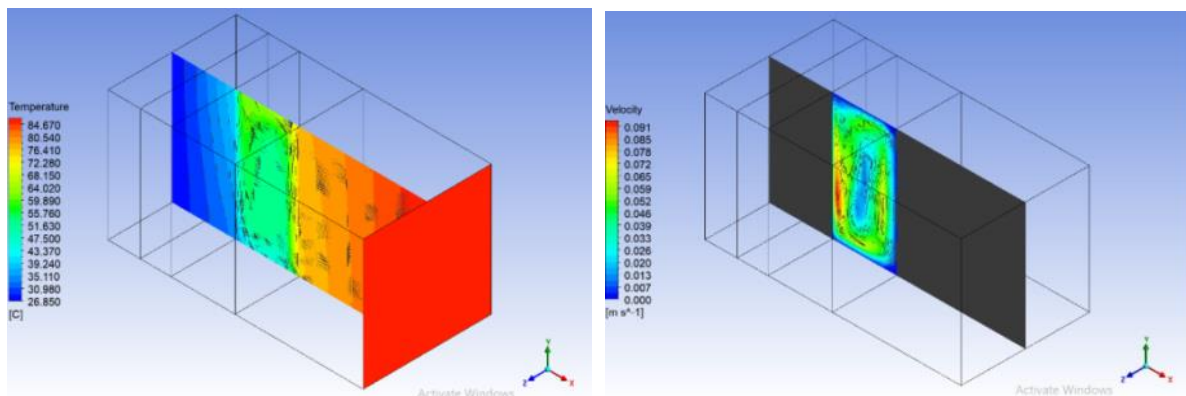
where $t_{T_{in[max]}}$ and $t_{T_{in[min]}}$ are the maximum and minimum inside surface temperatures,

respectively, and $t_{T_{out[max]}}$ and $t_{T_{out[min]}}$ are the maximum and minimum outside surface temperatures, respectively.

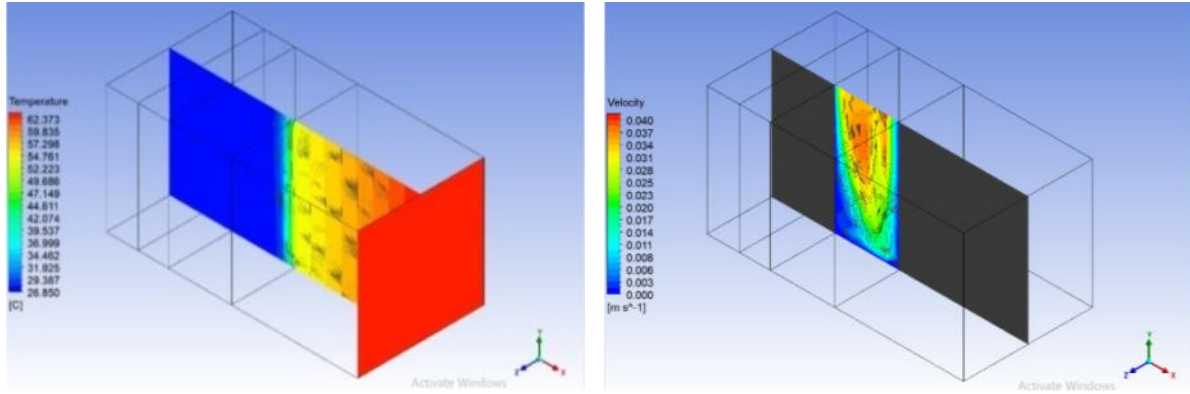
4.RESULTS AND DISCUSSION

4.1.Numerical Investigation

Figure 3 shows the temperature and velocity distribution through the wall without holes. The maximum temperature was 84.670 °C, and the maximum velocity was 0.091 m/sec. However, using an opening air gap decreased the maximum temperature to 62.363 °C and the maximum velocity to 0.04 m/sec. Fig. 4 shows the temperature and velocity distribution through a 10-hole wall with and without an air gap opening. Fig. 5 shows the temperature (left) and velocity (right) contours without opening the air gap. To study the effect of changing the dimensions of the holes on the maximum temperatures and velocity, the results showed that the 6-10-8 holes caused the minimum temperature of 65.442 °C, and the model of 6-8-10 holes caused the maximum temperature of 67.367 °C. The closed air gap increased the air circulation inside the wall cavity, increasing the heat transfer by convection and conduction to the inner wall. The maximum velocity was near the holes' inlet, where the hot air exited from the holes. The models of 6-8-10 holes and 10-8-6 holes caused the maximum velocity compared to other models. Fig. 6 presents the effect of an open cavity. The opening cavity would increase the wall thermal insulation because the heat exited from the air cavity by convection. The model of 8-10-6 holes caused a minimum temperature of 51.722 °C. However, the maximum temperature existed from the model of 6-10-8 holes, which will give a minimum temperature of 51.722 °C a maximum temperature of 51.881 °C. The cavity opening cooled the inner wall and increased the wall's thermal insulation. The results showed that holes in the wall increased the heat extraction from the wall, increasing the wall's thermal insulation.

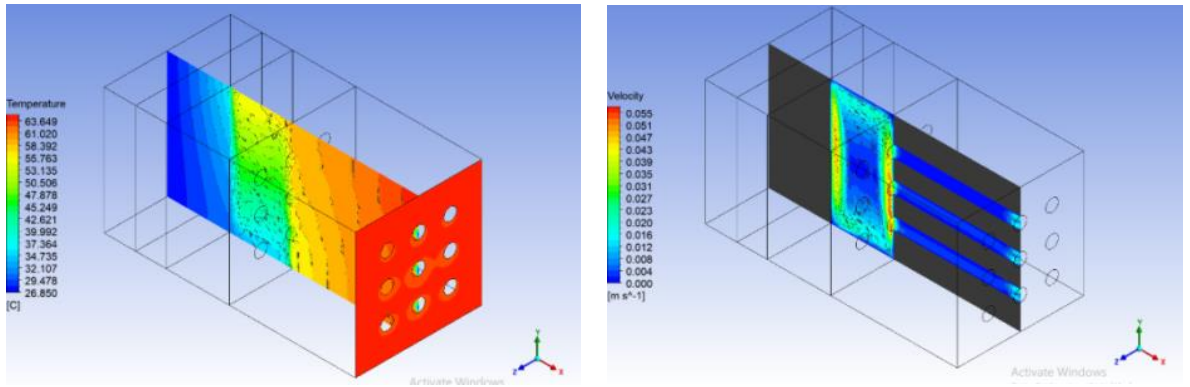


(a) Without Opening

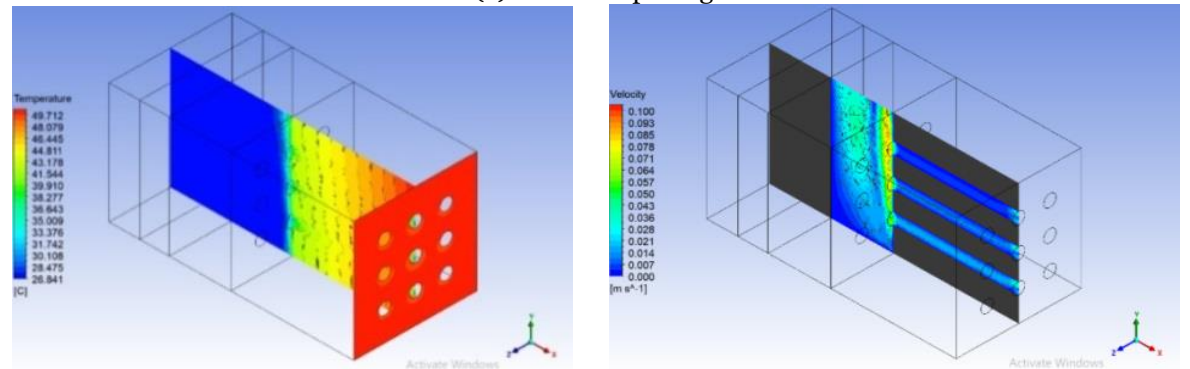


(b) With Opening

Fig. 3 Temperature and Velocity Contours Inside the Composed Wall Section Without and with Air Gap Openings and Without Holes.

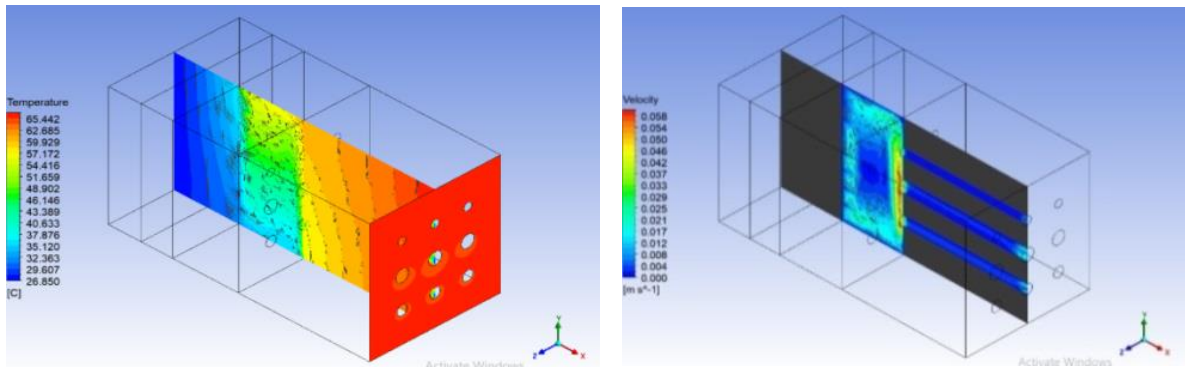


(a) Without opening

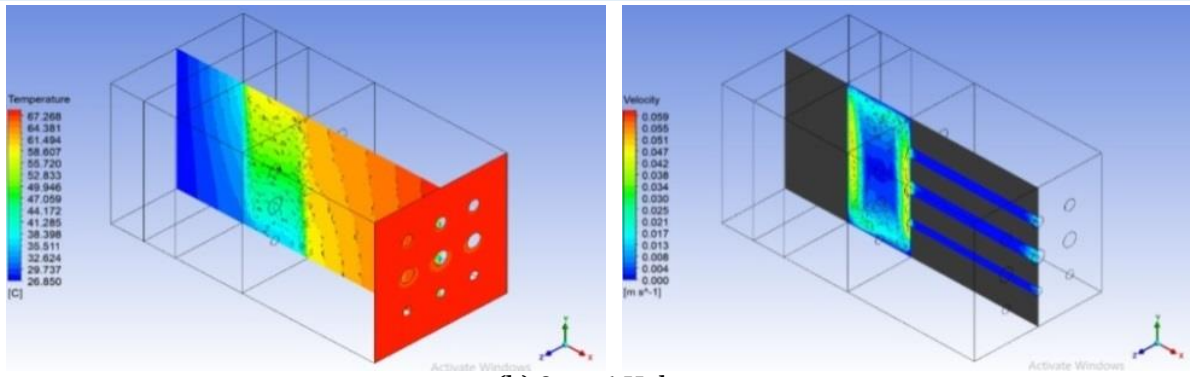


(b) With opening

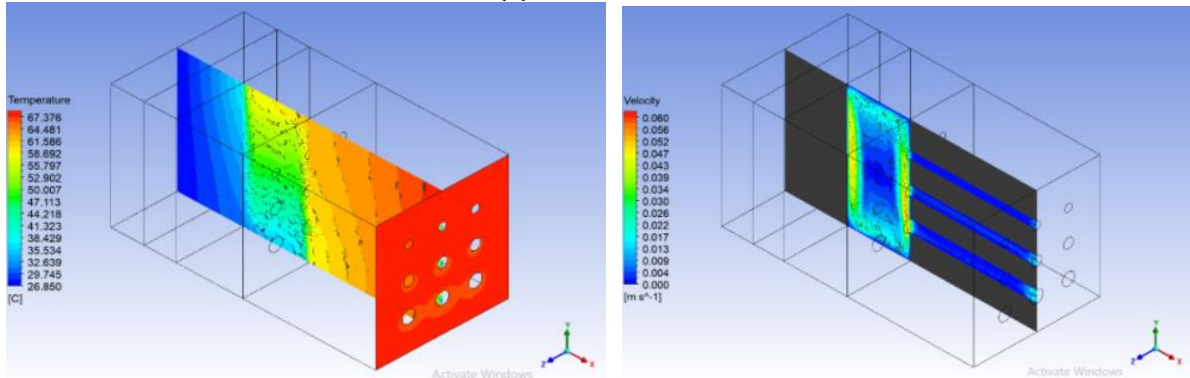
Fig. 4 Temperature and Velocity Contours Inside the Composed Wall Section with an Air Gap Opening and with 10 Holes Only.



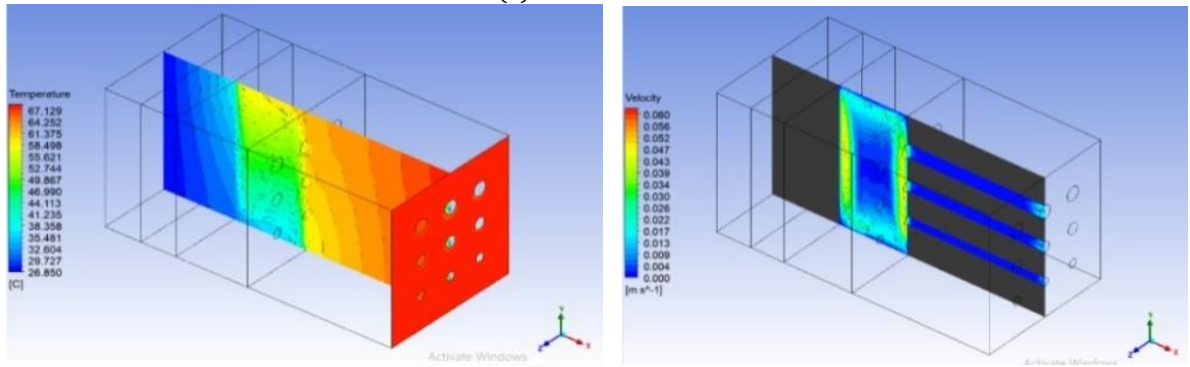
(a) 6-10-8 Holes



(b) 8-10-6 Holes

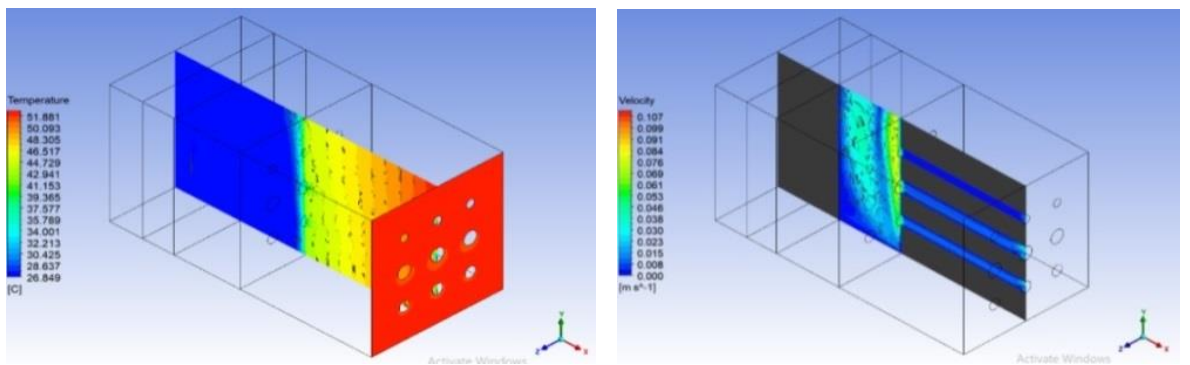


(c) 6-8-10 Holes



(d) 10-8-6 Holes

Fig. 5 Temperature and Velocity Contour Inside the Composed Wall Section Without Air Gap Opening.



(a) 6-10-8 Holes

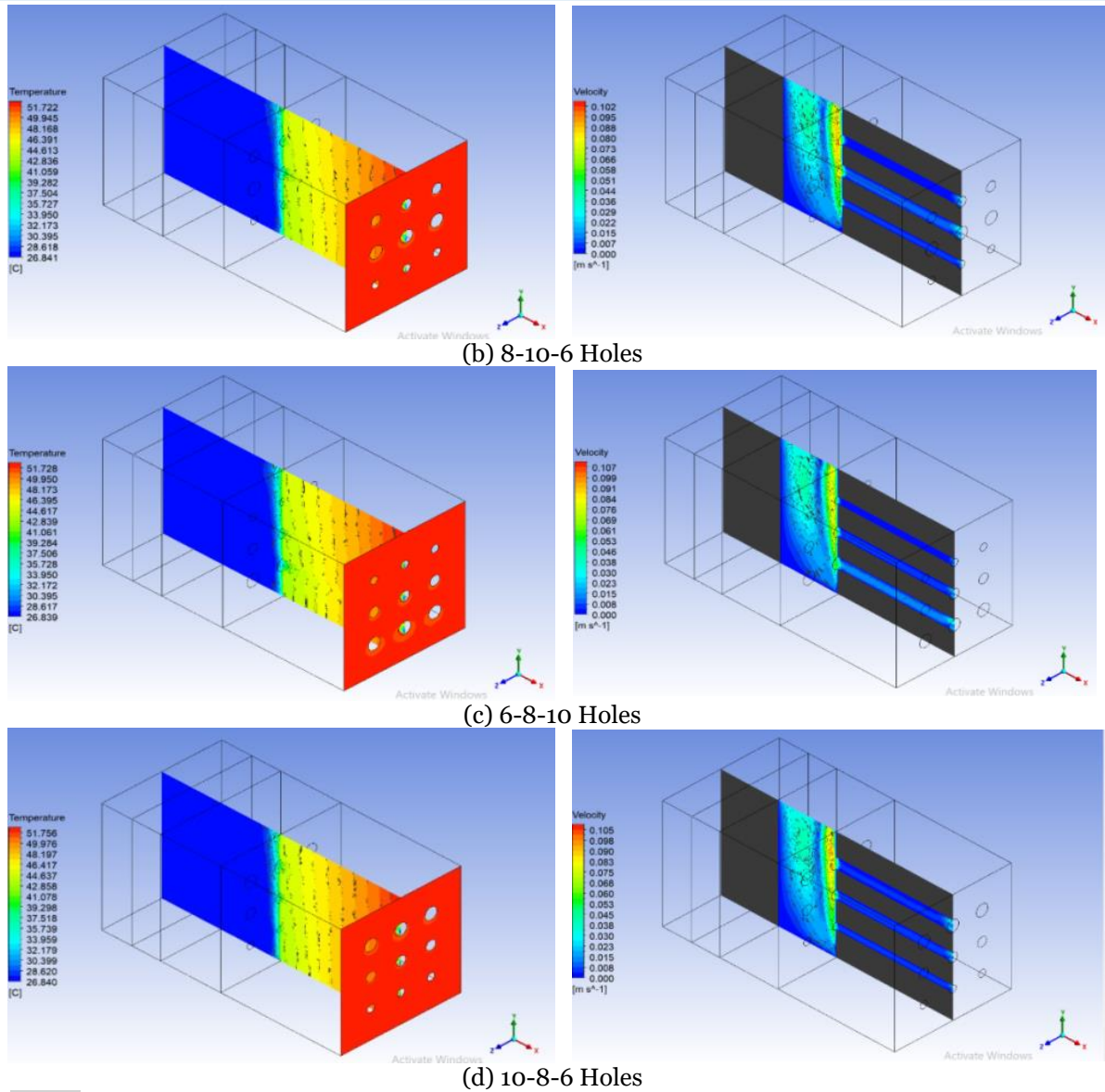


Fig. 6 Temperature and Velocity Contours Inside the Composed Wall Section with an Air Opening.

4.2. Experimental Investigation

4.2.1. Thermal Characteristics

Table 2 shows that the conventional model's overall heat transfer coefficient (U) value is 2.311 W/m².K. While the proposed models had less overall heat transfer, i.e., 1.920 W/m².K for Model A1, 2.01 W/m².K for Model A2, 1.720 W/m².K for Model B1, and 1.890 W/m².K for Model B2. The holes in the concrete block model consisting of the outer finishing material led to the recirculation of environmental air inside these blocks through the holes to the existing air gap between these concrete blocks and the building wall. The reduction percentages compared to the traditional wall were 17%, 13%, 26%, and 18%, respectively. According to Fig. 7, the thermal delay time for the conventional wall was 2:30 hours, and the thermal decrement factor was 0.4, while the thermal delay time increased to 4:0, 3:30, 5:25, and 4:30 hours for the A1, A2, B1, and B2 models, respectively. The thermal decrement factors were 0.49, 0.46, 0.53, and 0.51 for the

A1, A2, B1, and B2 models, respectively. The benefit of penetrated concrete block holes that form the finishing cover layer of the wall was the low density, which was in the 10% range, i.e., the solid block density was about 2000 kg/m³, while the perforated blocks were 1800 kg/m³. Another benefit was reducing the heat gained from the environmental impact by reducing the overall heat transfer coefficient (U) and increasing the thermal load decrement factor and delay time.

Table 2 Time lag, Decrement Factor, and U Value for the Studied Wall.

Studied Wall	Time Lag* (Hour)	Decrement Factor*	Overall Heat Transfer Coefficient** (U) w/m ² . K
Traditional Wall (Solid)	2:30	0.40	2.311
Model A1	4:00	0.49	1.920
Model A2	3:30	0.46	2.01
Model B1	5:25	0.53	1.720
Model B2	4:30	0.51	1.890

*All values were obtained from Fig. 7.

**All values were measured in the thermal test room at the Institute of Technology in Baghdad, Iraq.

4.2.2. Thermal Behavior of Concrete Models

To reach the goal of the research, an experimental study was conducted of the conventional wall (a solid block) and the four proposed models (A1, A2, B2, and B1), as shown in Fig. 2. The thermal behavior of these blocks was studied from 6 a.m. to 6 p.m. on the 21st of every month from May to September. The surface temperature of the wall facing the environment (T_o) and the temperature of the wall layer facing the room air (T_r) were recorded. The thermal behavior for June is shown in Fig. 7. Because the test wall faced the east, the wall surface temperature (T_o) reached its highest values between 9 a.m. and 10 a.m. when solar radiation was perpendicular to the wall. Meanwhile, the heat absorbed by the outer layer facing the environment continued to flow to the components of the wall layers. It reached the room space until the room air temperature increased and the time of its occurrence increased. Table 2 shows the delay time of the test wall thermal behavior. Also, the change in the environmental air temperature (shade) was recorded during the same period, where the maximum temperature was achieved at 3:00 p.m. The experiments were repeated according to the nature of the air gap between the perforated concrete blocks and the original wall of the building. Fig. 8 shows the daily average change during June for the wall surface temperatures (T_o), the inner surface temperature (T_i), and the temperature difference (ΔT_{o-i}) and (ΔT_{i-r}) after applying the four models with the principle of closing and opening the air gap between the original wall of the building and the perforated wall. Fig. 9 shows the seasonal average (over the summer season) of the surface temperatures facing the room space and the temperature difference ΔT_{i-o} and ΔT_{i-r} for the models of the walls under study and according to the condition of the air gap.

4.2.3. Surface Temperatures and Temperature Differences (T_i , T_o , ΔT_{o-i} , and ΔT_{o-r})

The building blocks' thermal resistance that comprises the outer covering layer works to dampen the frequency of heat affected by the environment; however, it is eventually reflected in the internal surface temperature of this layer (T_i) value. Fig. 8 shows that the conventional wall average temperatures of exterior and interior surfaces were 45.9 and 40.1 °C,

respectively. The corresponding temperatures of the perforated concrete blocks in models A1, A2, B1, and B2 measured with a closing air gap were (43.74, 39.76), (43.3, 39.54), (42.82, 39.1), and (44.34, 39.68) °C, respectively. The influence of ambient air circulation via the outside covering materials decreased the block temperature, as indicated by the inner and outer wall surfaces temperatures. The temperature difference between the outside and inside surface temperatures (ΔT_{i-o}) was 5.8 °C for the conventional wall and 3.76, 3.26, 3.72, and 3.31 °C for models A1, A2, B1, and B2, respectively. The effect is clear on the ΔT_{i-r} value, i.e., 13.26, 13.04, 12.6, and 13.18 °C for models B2, B1, A2, and A1, compared with the conventional wall that was recorded (14.6 °C), as shown in Fig. 9. Due to the environmental air movement around the perforated wall materials (models), it was possible to leak a portion of the heat stored in that mass, decreasing its thermal level, which decreased the heat transferred to the layers of the wall towards the air-conditioned room.

4.3. Opening Mode Results

The thermal behavior of a wall with an air gap separating the outside finishing layer (perforated concrete blocks) and the main building wall was investigated in three modes: a normally closed air gap system, a normally opened air gap system, and an opened air gap at night with a closed air gap during the day. For model A1, the temperature difference between the interior surface facing the room space and the design room air temperature (ΔT_{i-r}) was 13.26 °C when the gap was entirely closed and 14.43 °C when the gap was constantly open to the environment, as shown in Fig. 8. When the gap was opened at night and closed during the day, the temperature difference decreased to 13.13 °C. It is considered the most efficient mode because opening the gap at night allows relatively cold and moist environmental air to pass through the holes of the concrete blocks, passing through the gap behind the concrete blocks to the outside of the wall. Thus, it effectively absorbs the heat accumulated in the gap and its sides and convects it outside the system. As a result, the air temperature maintained within the gap dropped before it was closed again, i.e., night gap ventilation minimized the heat transferred into the conditioned room.

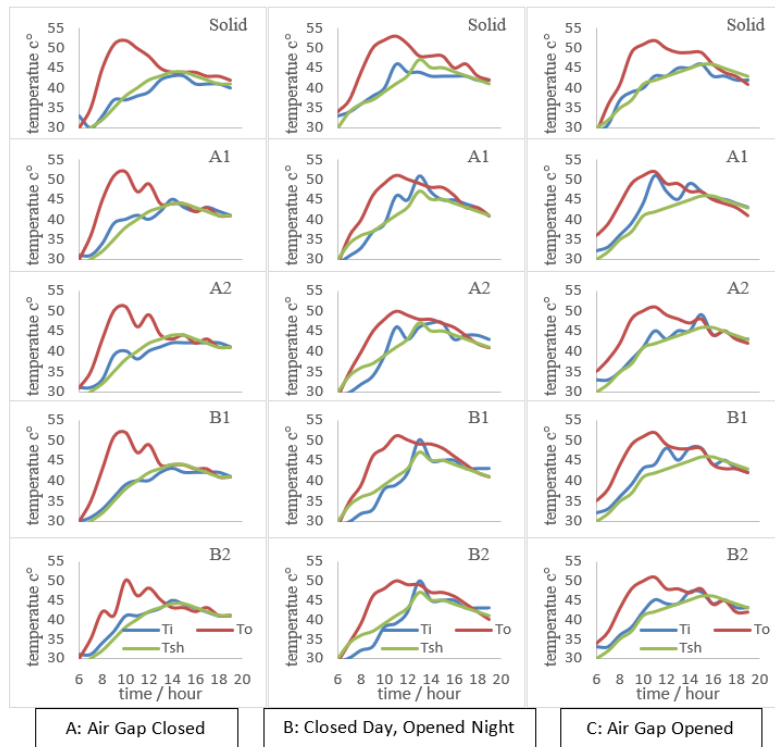


Fig. 7 Hourly Thermal Behavior of All Studied Walls in June.

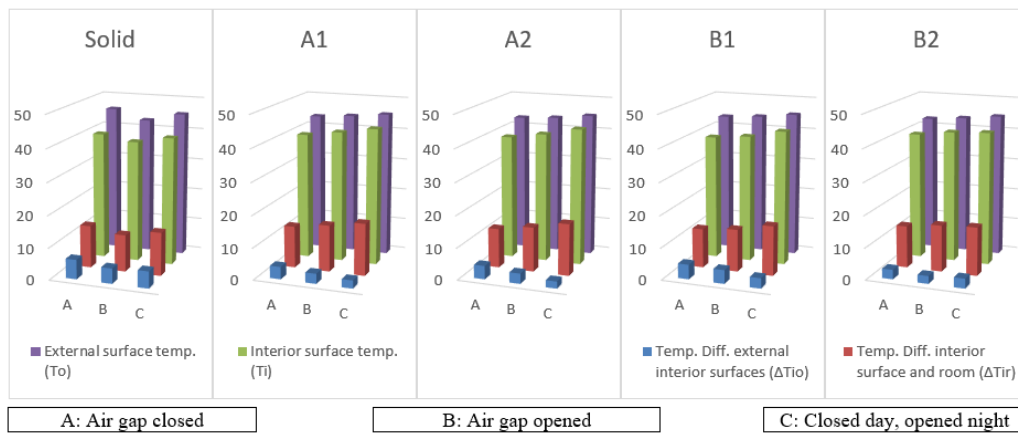


Fig. 8 Temperature Values of Wall Surfaces for All Studied Cases in June.

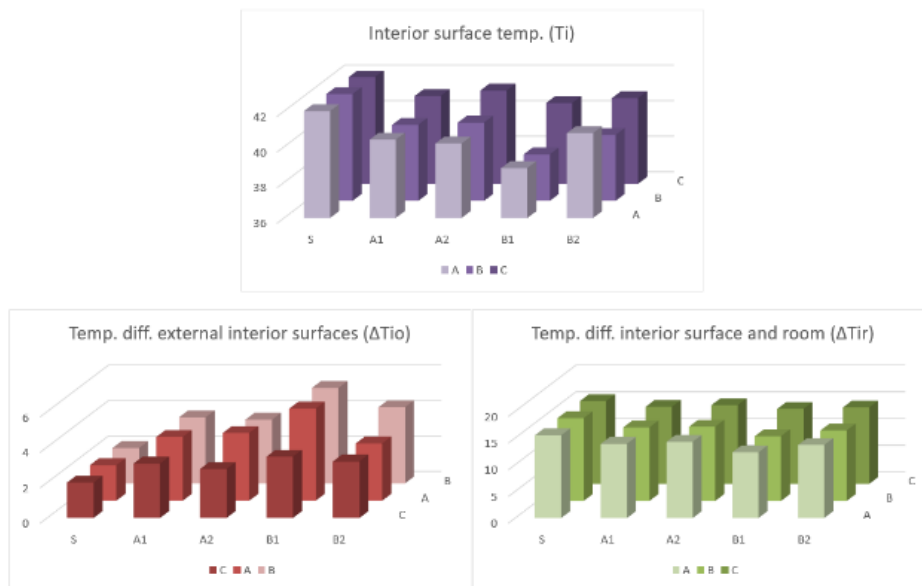


Fig. 9 Seasonally Averaged Temperature Values of The Wall Surface.

4.4. Energy Consumption and Energy Savings

The energy-hour meter was directly connected to the electrical circuit of the air conditioner to accurately measure the energy consumption during the air conditioner's operational period. Fig. 10 shows that the electric power consumed by the air conditioner to provide the standard thermal conditions in the test room with the conventional model (using solid model concrete blocks to cover the wall) was 98.5 kilowatt-hours. In contrast, the four perforated concrete blocks models recorded energy consumption values of 87.5 kilowatt-hours, representing an 11.2% reduction compared to the conventional solid model for model A1, model A2 recorded 83.9 kilowatt-hours, representing a 15% reduction, model B2

recorded 80 kilowatt-hours, representing a 19% reduction, and model B1 recorded 78 kilowatt-hours, representing a 21% reduction, in the case of the gap being open at night and closed during the day.

4.5. Thermal Performance of Blocks Perforated with Variable and Constant Diameters

Hasan et al. [28] studied the thermal behavior of cement blocks perforated with nine holes of constant diameters and identified that the block with diameters of 6 mm was the most thermally efficient and achieved an electrical energy saving percentage (to provide comfortable thermal conditions within the space) of about 22.82%, which was higher than blocks with nine holes and variable diameters studied in the present work.

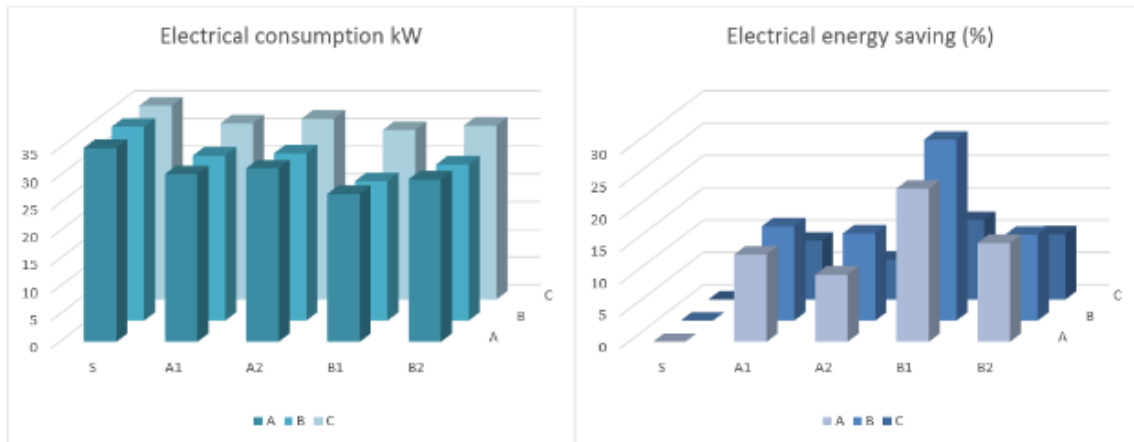


Fig. 10 Annual Electrical Energy Consumption (kW) and Percentage Savings (%).

5. CONCLUSIONS

5.1. Numerical

- Using an opening air gap decreased the minimum temperature to 62.363 °C and the minimum velocity to 0.04 m/sec. The 6-10-8 holes model caused the minimum temperature of 65.442 °C, and the 6-8-10 holes model caused the maximum temperature of 67.367 °C.
- In the closed air gap mode, the models of 6-8-10 holes and 10-8-6 holes caused the maximum velocity compared to other models.
- For an open cavity, the model of 8-10-6 holes caused a minimum temperature of 51.722 °C; however, the maximum exist temperature from the 6-10-8 holes model was 51.881 °C.

5.2. Experimental

- The reduction percentages of the coefficient (U) from the conventional model were 17, 13, 26, and 18% for A1, A2, B1, and B2, respectively.
- The thermal delay time increased to 4:0, 3:30, 5:25, and 4:30 hours for the A1, A2, B1, and B2 models, respectively,

compared to a conventional wall of 2:30 hours. The thermal decrement factor was 0.49, 0.46, 0.53, and 0.51 for the A1, A2, B1, and B2 models under evaluation, respectively, compared to the conventional wall thermal decrement factor of 0.4.

- T_o and T_i recorded for model A1 were (43.74, 39.76) °C, A2 were (39.54, 43.3) °C, B1 were (42.82, 39.1) °C, and B1 and B2 recorded (42.82, 39.1) °C and (44.34, 39.68) °C, respectively, compared to the conventional wall of (45.9, 40.1) °C.
- ΔT_{i-o} of the conventional wall was 5.8 °C while about 3.76, 3.26, 3.72, and 3.31 °C were recorded for A1, A2, B1, and B2, respectively.
- ΔT_{i-r} was 13.26, 13.04, 12.6, and 13.18 °C for models B2, B1, A2, and A1, respectively. As the air gap between the outer finishing layer of perforated concrete blocks and the main wall of the test room was closed, a (14.6) °C decrease was observed compared to the conventional wall.
- For model A1, ΔT_{i-r} was 13.26 °C when the gap was entirely closed and 14.43

- °C when the gap was constantly open to the environment. When the gap was opened at night and closed during the day, ΔT_{i-r} decreased to 13.13 °C.
- 7- ΔT_{i-r} in the case of a closed gap and according to the model sequence (B2, B1, A2, A1) was (13.26, 13.04, 12.6, 13.18) °C. When the gap was open to the environmental air at 14.44, 14.43, 13.61, and 13.84 °C, in the case of the gap being open at night and closed during the day, the values were 13.13, 12.83, 12.05, and 12.15 °C, respectively.
- 8- The conventional solid model (using solid model concrete blocks) consumed 98.5 kilowatt-hours of electrical energy, representing an 11.2% reduction compared to the conventional solid model for model A1, model A2, representing a 15% reduction, model B2, representing a 19% reduction, and model B1, representing a 21% reduction, in the case of the gap being open at night and closed during the day.

NOMENCLATURE

μ	Dynamic viscosity (Pa.s ⁻¹)
C_p	Specific heat (J.kg ⁻¹ .K ⁻¹)
U	Velocity in x-direction (m.s ⁻¹)
P	Pressure (Pas)
g	Gravity acceleration (m.s ⁻²)
t	Time(s)
k	Thermal conductivity (w.m ⁻¹ .k ⁻¹)
v	Velocity in y-direction (m.s ⁻¹)

REFERENCES

- [1] Kontoleon KJ, Theodosiou TG, Tsikaloudaki KG. **The Influence of Concrete Density and Conductivity on Walls' Thermal Inertia Parameters under a Variety of Masonry and Insulation Placements.** *Applied Energy* 2013; **112**: 325–337.
- [2] Chua KJ, Chou SK, Yang WM, Yan J. **Achieving Better Energy-Efficient Air Conditioning - A Review of Technologies and Strategies.** *Applied Energy* 2013; **104**: 87–104.
- [3] Hasan AA. **Thermal Conductivity of Building Materials in Iraq.** *Tikrit Journal of Engineering Science* 2021; **28**: 37–49.
- [4] Waes MM. **Optimum Building Wall Thickness under Actual Weather Conditions for Kirkuk City.** *Tikrit Journal of Engineering Sciences* 2018; **25**(4): 11–15.
- [5] Schiavoni S, Bianchi F, Asdrubali F, others. **Insulation Materials for the Building Sector: A Review and Comparative Analysis.** *Renewable and Sustainable Energy Reviews* 2016; **62**: 988–1011.
- [6] Mohamed M, Almarshadi M. **Energy Saving in Air Conditioning of Buildings.** *MATEC Web of Conferences* 2018; **162**: 5024, (1-5).
- [7] Xing G, Yu J, Zhang C, Wu JX. **A New Energy-Efficient Building System Based on Insulated Concrete Perforated Brick with A Sandwich.** *Civil Engineering Journal* 2018; **4**(7): 1467-1476.
- [8] Iffa E, Tariku F, Simpson WY. **Highly Insulated Wall Systems with Exterior Insulation of Polyisocyanurate under Different Facer Materials: Material Characterization and Long-Term Hygrothermal Performance Assessment.** *Materials* 2020; **13**(15): 3373.
- [9] Dafalla MA, Al Shuraim MI. **Efficiency of Polystyrene Insulated Cement Blocks in Arid Regions.** *GEOMATE Journal* 2017; **13**(36): 35–38.
- [10] Hasan AA, Aljawad RH, Jehhe KA. **Experimental and Numerical Study of Thermal Performance and Energy Saving by Using Hollow Limestone Walls.** *Sc Bull, Series D* 2019; **81**(4): 301–312.
- [11] Mahlia TMI, Iqbal A. **Cost Benefits Analysis and Emission Reductions of Optimum Thickness and Air Gaps for Selected Insulation Materials for Building Walls in Maldives.** *Energy* 2010; **35**(5): 2242–2250.
- [12] Fraisse G, Johannes K, Trillat-Berdal V, Achard G. **The Use of a Heavy Internal Wall with a Ventilated Air Gap to Store Solar Energy and Improve Summer Comfort in Timber Frame Houses.** *Energy and Buildings* 2006; **38**(4): 293–302.
- [13] Ahuja A, Mosalam KM. **Evaluating Energy Consumption Saving from Translucent Concrete Building Envelope.** *Energy and Buildings* 2017; **153**: 448–460.
- [14] Yükses İ. **The Evaluation of Building Materials in Terms of Energy Efficiency.** *Periodica Polytechnica Civil Engineering* 2015; **59**(1): 45–58.
- [15] Faraj RH, Ali HFH, Sherwani AFH, Hassan BR, Karim H. **Use of Recycled Plastic in Self-Compacting Concrete: A Comprehensive Review on Fresh and Mechanical Properties.** *Journal of Building Engineering* 2020; **30**: 101283.
- [16] Faraj RH, Sherwani AFH, Jafer LH, Ibrahim DF. **Rheological Behavior**

- and Fresh Properties of Self-Compacting High Strength Concrete Containing Recycled PP Particles with Fly Ash and Silica Fume Blended.** *Journal of Building Engineering* 2021; **34**: 101667.
- [17] Machado AL, Schneider RM, do Amaral AG. **Soil-Cement Bricks as an Alternative for Glass Waste Disposal.** *American Scientific Research Journal for Engineering, Technology, and Sciences* 2020; **71**(1): 123–135.
- [18] Amaral MC, Siqueira FB, Destefani AZ, Holanda JNF. **Soil--Cement Bricks Incorporated with Eggshell Waste.** *Proceedings of the Institution of Civil Engineers-Waste and Resource Management* 2013; **166**(3) :137–141.
- [19] Ahmed H, Ibrahim IM, Radwan MA, Sadek MA, Elazab HA. **Preparation and Analysis of Cement Bricks Based on Rice Straw.** *International Journal of Emerging Trends in Engineering Research* 2020; **8**(10): 7393–7403.
- [20] Kongkajun N, Laitila EA, Ineure P, Prakaypan W, Cherdhirunkorn B, Chakartnarodom P. **Soil-Cement Bricks Produced from Local Clay Brick Waste and Soft Sludge from Fiber Cement Production.** *Case Studies in Construction Materials* 2020; **13**: e00448, (1-10).
- [21] Khaleel MH. **Thermal Loads and Cost Reduction for a Residential House by Change Its Orientation and Add Roof Shading.** *Tikrit Journal of Engineering Sciences* 2020; **27**(4): 13–30.
- [22] Ramesh N, Merzkirch W. **Combined Convective and Radiative Heat Transfer in Side-Vented Open Cavities.** *International Journal of Heat and Fluid Flow* 2001; **22**(2): 180–187.
- [23] Launder BE, Spalding DB. **Lectures in Mathematical Models of Turbulence.** New York: Academic Press; 1972.
- [24] Fluent A. **Ansys Fluent Theory Guide.** *Ansys Inc. USA* 2011; **15317**: 724-746.
- [25] Pletcher RH, Tannehill JC, Anderson D. **Computational Fluid Mechanics and Heat Transfer.** 3rd ed., New York: CRC Press; 2012.
- [26] Versteeg HK. Malalasekera, **An Introduction to Computational Fluid Dynamics. The Finite Volume Method.** *Willey, New York* 1995.
- [27] Rohsenow WM, Hartnett JP, Cho YI. **Handbook of Heat Transfer.** 3rd ed., USA: McGraw-Hill; 1998.
- [28] Hasan AA, Al-Bayati OAZ, Aljawad RH. **the Reducing of Building Cooling Load by Using the Drilled Cement Mortar as a Finishing Material.** *UPB Scientific Bulletin, Series D: Mechanical Engineering* 2022; **84**(1): 149–162.